Modeling convective heat transfer augmentation of TiO_2 nanofluids using neural networks

Abstract

In this study, neural network method was employed to estimate forced convective heat transfer coefficient of nanofluids. Solutions with different TiO_2 nanoparticle concentrations were synthesized using the two-step method and flowed upward through a vertical pipe in laminar and turbulent flow regimes. Different operational parameters such as heat flux, thermal conductivity of fluids, nanoparticle concentration and flow Reynolds number were performed to measure the convective heat transfer coefficient. In order to model convective heat transfer coefficient, these operational parameters introduce to artificial neural network as inputs. Static factors such as mean square error and correlation coefficient were determined and indicate high performance of ANN in modeling this process. Addition of nanoparticles into the base fluid, enhances the forced convective heat transfer coefficient of fluid and this effect is more considerable in base fluids with lower thermal conductivity and flow with higher Reynolds number and higher heat fluxes..............................

Keywords: Nanofluids; Forced convection; artificial neural networks; TiO_2 nanoparticles

1.Introduction

Improving efficiency of working fluid in thermo systems enhances the efficiency of them and minimizes their size. Taking advantage of nanofluids has been considered as an excellent approach for this. Nanofluid, the suspension of small percent (<5 vol. %) various types of nanoparticles into conventional working fluids, can solve the problems of working fluids with poor thermal properties in advanced heat transfer systems.

In one Study by Pak and Cho on Nanofluid consist of 3 vol. % 27 nm titanium dioxide particle in water, a new correlation for the turbulent convective heat transfer for dilute concentration of nanofluids are reported as follows [1]:

$$\mathrm{Nu} = 0.021\mathrm{Re}^{0.8}\mathrm{Pr}^{0.5} \qquad \text{for} \qquad 6.54 \le \mathrm{Pr} \le 12.33 \quad 10^4 \le \mathrm{Re} \le 10^5 \qquad (1)$$

Stable aqueous 20 nm titanium dioxide with different agglomerate sizes and concentration are synthesized by He et.al. They showed convective heat transfer coefficient increases with nanoparticle concentration and reported the higher effects in the turbulent flow regime. In the other study, They compared this data with numerical results and a good agreement was achieved [2].

More than experimental study is desirable to model the process and find empirical relations between effective parameters. Artificial neural network in the last decade were used to model different applicable process.

A. K. Santra, et. al studied Heat transfer due to laminar natural convection of copper–water nanofluid as a non-Newtonian fluid in a differentially heated square cavity by Artificial Neural Network (ANN). The ANN has been trained by a resilient-propagation (RPROP) algorithm. It has been observed that the ANN predicts the heat transfer correctly within the given range of training data [3].

Fazeli, et al. studied the heat transfer characteristics of a miniature heat sink cooled by SiO_2–water nanofluids experimentally and numerically. An artificial neural network (ANN) was used to simulate the heat sink performance. It was found that the results of ANN are in excellent agreement with the mathematical simulation and cover a wider range for evaluation of heat sink performance [4].

M. Balcilar, et al. determine the important parameters' effects on the heat transfer coefficient of Nanofluids with various concentrations and also to have reliable empirical correlations based on the neural network (ANNs) analysis. The performance of the method of MLP with 10-20-1 architecture, GRNN with the spread coefficient 0.7 and RBFs with the spread coefficient of 1000 and a hidden layer neuron number of 80 are found to be in good agreement, predicting the experimental pool boiling heat transfer coefficient with deviations within the range of ±5% for all tested conditions [5].

M. M. Papari et. al employed neural network analysis to estimate thermal conductivity of nanofluids consisting of multi-walled carbon nanotubes (MWCNTs) and single-walled carbon nanotubes (SWCNTs) suspended in different types of fluids. The results obtained have been compared with other theoretical models as well as experimental values. The predicted thermal conductivities are in good agreement with the literature values [6].

M. Hojjat et. al synthesized three different types of nanofluids by dispersing γ-Al_2O_3, TiO_2 and CuO nanoparticles in a 0.5 wt% of carboxymethyl cellulose (CMC) aqueous solution. Thermal conductivity of nanofluids were measured experimentally. Results show that the increase in the thermal conductivity varies exponentially with the nanoparticle concentration and temperature. Neural network models were proposed to represent the thermal conductivity as a function of the temperature, nanoparticle concentration and the thermal conductivity of the nanoparticles. These models were in good agreement with the experimental data [7].

In this paper, we have used neural network to estimate forced convective heat transfer coefficient of nanofluids. The objective of this study is to compare the results of this modeling with experimental data are obtained for water and ethylene glycol/water mixture as base fluid. Nanofluids containing TiO_2 nanoparticles of various concentrations will be tested under the different heat flux boundary conditions in flowing upward through a vertical pipe in laminar and turbulent flow regimes.

2. Experimental

Spherical titanium dioxide nanoparticles dispersed in distilled water and ethylene glycol/water mixture (60 weight-% ethylene glycol). Nanoparticles were purchased from Degussa (Germany) with an average diameter of 25 nm. Ultrasonic vibrator (Tecna 6) was used for preparation of mixed aqueous suspensions. Suspension were sonicated for 4 hours at a frequency of 50-60 kHz with an output power of 138W, at 65ºC and pH=11 by NaOH solution. Nanofluids containing 0.5%, 1.0%, 1.5% titanium dioxide by volume were obtained by using the above method that was known as two step method. Stability time of nanofluids was observed 24 hours without any stabilizer in this work..

The test section in Fig.1 (experimental apparatus) was a straight copper tube with length of 120 cm, inner diameter of 6 mm and outer diameter of 8 mm. Two rod of heaters with different AC power in parallel with the tube were used as heaters with Thick thermal isolating layer.

Four (K- type) thermocouples were welded on inner tube wall at 20 cm (T_{w1}), 50 cm (T_{w2}), 80 cm (T_{w3}) and 110 cm (T_{w4}) from the inlet of the test section. Two further K-type thermocouples were inserted into the flow at 8 cm (T_{fin}) and 119 cm (T_{fout}) from the inlet of the test section.

After injection of nanofluid in a glass vessel as fluid reservoir tank, it was circulated toward the test section using a pump (STAR RS 25/6-130). Flow rate was measured by a flow meter and different flow rate (0.5- 5.0 L/min) was obtained by using a valve before the flow meter.

To cool nanofluids a tube-in-shell type heat exchanger was used.

2-1- Problem formulation

The experimental data was used for calculation of the convective heat transfer coefficient (h) and Nusselt number as follows:

$$h_f(x) = \frac{q}{(T_w(x) - T_f(x))} \tag{2}$$

q is the heat flux, T_w is the measured wall temperature, and T_f is the fluid temperature calculated by the following energy balance equation:

$$T_f(x) = T_{fin} + qSx/\rho_f c_f Q \tag{3}$$

where T_{fin} is the measured fluid temperature at inlet of the test section, c_f is the fluid heat capacity, ρ_f is the fluid density, S is perimeter of the test tube and Q is the flow rate. For nanofluid, the value of (ρc) was calculated by the following equation:

$$(\rho c)_{nf} = \varphi(\rho c)_p + (1 - \varphi)(\rho c)_f \tag{4}$$

The measured temperature of fluid at the outlet of the test section was compared with the theoretical value calculated by Eq. (3), it was found that the maximum deviation was lower than 12% under the conditions of this work.

The convective heat transfer coefficient, h, in Eq. (2) is usually expressed in the form of the Nusselt number (Nu) as:

$$Nu_f(x) = \frac{h_f(x)D}{k_f} \tag{5}$$

where D is the tube inner diameter and k_f is the fluid thermal conductivity and for nanofluid is predicted by the H-C model, [8]:

$$\frac{k_{nf}}{k_f} = \left[\frac{k_p + (n-1)k_f + (n-1)\varphi(k_p - k_f)}{k_p + (n-1)k_f + \varphi(k_p - k_f)}\right] \tag{6}$$

where n is the shape factor given by n = 3/ψ with ψ the sphericity (ψ = 1 for spherical particles). k_f and k_p are the thermal conductivities of the base fluid and particles, respectively. Traditionally, the Nu number is related to the Reynolds number defined as $Re = \rho_f uD/\mu_f$ and the Prandtl number defined as $Pr = \upsilon/\alpha$, where υ is the fluid kinematic viscosity, α is the fluid thermal diffusivity and μ_f is the fluid dynamic viscosity and for nanofluid is predicted by the Einstein equation $\mu_{nf} = \mu_f (1 + 2.5\varphi)$. In Eq. (5) x represents axial distance from the entrance of the test section

3- Modeling

In this study, an ANN program was written in the environment of MATLAB software. A total of 56 experimental datasets, which were obtained from different experiments, were used to develop a three-layer feed-forward neural network model. The hyperbolic tangent sigmoid (tansig) transfer function with a back-propagation algorithm at the hidden layer and a linear transfer function (purelin) at the output layer were applied. In order to increase the numerical stability (accuracy index) of the model construction, the inputs and the target were first normalized to produce data with zero mean and unity standard deviation, and then the principal component analysis was performed before the training stage. It was observed that the number of principal components, which accounted for 98 % of the variation, is equal to the number of original input parameters and there was no redundancy in the dataset. In the next step, the datasets were divided into three different sets: a training dataset with one-half of the data for training the ANN; a validation data-set with one-quarter of the data for validating the developed ANN; and a testing set with one-quarter of the data for testing the ANN. The division of the datasets was followed by performing various learning algorithms to select the best one. Finally, the optimization was carried out between the neuron number and MSE for the best learning algorithm. In this work, different types of statistical parameters such as mean absolute error (MAE), mean squared error (MSE), root mean squared error

(RMSE), and determination coefficient (R^2) were calculated to estimate the accuracy of the process.

4- Results and discussion

4-1- Learning algorithm selection

In order to select the best back-propagation learning algorithm, different types of learning algorithm were performed. A three-layer feed-forward ANN with a tansig transfer function at the hidden layer and a purelin transfer function at the output layer was used for all the back-propagation learning algorithms. For all the algorithms, 10 neurons were used in the hidden layer. The results are given in Table 1.

As can be seen, the Levenberg–Marquardt (LM) algorithm with the minimum MSE of 0.0010 was found as the best back-propagation learning algorithm.

4-2- Optimization of artificial neural network

The number of hidden layer neurons is an essential parameter affecting the performance of ANNs. If the value is set too low, the network would not be trained properly, and if it is set too high, the network would be over-trained [11]. In this study, the best number of neurons in the hidden layer was determined by the trial and error method in which the number of neurons was varied from 2 to 9. The relationship between the number of neurons in the hidden layer and MSE are reported in Table 2. The minimum MSE value of 0.0008 is observed for 6 neurons in the hidden layer. Therefore, the ANN was designed with 6 neurons in the hidden layer.

4-2Convective heat transfer coefficient of distilled water

The experimental system was tested with distilled water at two Reynolds number of 2960 and 3960. To check the constant heat flux boundary condition in this work, the experimental data of convective heat transfer coefficient of distilled water in form of Nu number was compared with predicted Nu number from Gnielinski equation, [9], (See Figs. 2(a) and 2(b)). This equation under the constant heat flux boundary condition is as follows:

$$\mathrm{Nu} = \frac{\left(\frac{f}{2}\right)\left(\mathrm{Re} - 10^3\right)\mathrm{Pr}}{1 + 12.7\left(\frac{f}{2}\right)^{\frac{1}{2}}\left(\mathrm{Pr}^{\frac{2}{3}} - 1\right)}, \quad f = 0.078\,\mathrm{Re}^{-\frac{1}{4}}, \quad \begin{cases} 0.5 < \mathrm{Pr} < 10^6 \\ 2300 < \mathrm{Re} < 5\times10^6 \end{cases} \qquad (7)$$

The Gnielinski equation predicts the experimental data by 4% deviation for Re = 2960 and 3% deviation for Re = 3960. These deviations are due to the effect of the entrance on heat transfer coefficient, which does not include in Eq. (7). Therefore, the boundary condition of constant heat flux for this study is valid.

4-3Effect of nanoparticle concentrations on the convective heat transfer coefficient in distilled water

In Figs. 3(a) and 3(b), experimental results and predicted data from ANN were compared. the axial profiles of the heat transfer coefficient of nanofluids increase with increasing particle concentration. The enhancement in the high Reynolds number is more than the low Reynolds number, namely, for example, at Re = 2960 and Re = 3960, the maximum enhancement with 1.50 vol. % TiO_2 nanofluids is about 40% (see Fig. 3(a)) and more than 52% (see Fig. 3(b)), respectivly. Good agreement between experimental results and predicted data shows high accuracy of ANN in predicting this process.

4-4Convective heat transfer coefficient of water/ethylene glycol mixture

The experimental system was tested with mixture consisting of 60 weight-% ethylene glycol and 40 weight-% distilled water at Re = 2030. Fig. 4 shows the measured data. This figure also compares the measured data with calculated values from Shah equation, [10].

Shah equation for the laminar flows under the constant heat flux boundary condition is as follows:

$$\mathrm{Nu}=\begin{cases}1.953\left(\mathrm{RePr}\dfrac{D}{x}\right)^{\frac{1}{3}} & \left(\mathrm{RePr}\dfrac{D}{x}\right)\geq 33.3\\ 4.364+0.0722\,\mathrm{RePr}\dfrac{D}{x} & \left(\mathrm{RePr}\dfrac{D}{x}\right)<33.3\end{cases} \qquad (8)$$

The Shah equation predicts the experimental data by 1.5% deviation for Re = 2030.

4-5Effect of nanoparticle concentration on the convective heat transfer coefficient in mixture of water and ethylene glycol

Fig. 5 shows the axial profiles of the convective heat transfer coefficient of nanofluids with different TiO_2 particle concentrations in the mixture consisting of 60 weight-% ethylene glycol and 40 weight-% distilled water at Re = 2030. The convective heat transfer coefficient was indicated on the base of experimental data and ANN results. This figure shows that with increasing particle concentration the convective heat transfer coefficient of TiO_2 increases.

4-6Effect of heat flux on the convective heat transfer coefficient of nanofluid

Fig. 6 shows enhancement of convective heat transfer coefficient for power supply of 440W and 550W on the base of experimental data and ANN results. In this figure the convective heat transfer coefficient in distilled water nanofluid increases with increasing heat flux. Results also show that the improvement of convective heat transfer coefficient of base fluid because of addition of nanoparticles seems to be more considerable in the turbulent flow regimes and higher heat fluxes. Comparing of experimental data and ANN results indicates that ANN could predict this process in lower heat flux better than higher one.

5-Conclusions

In this study, an experimental work has been carried out on the heat transfer behavior of TiO_2 nanofluids flowing through a straight vertical pipe under both the laminar and turbulent flow conditions. The results were used by ANN in order to model this process. effect of operational parameters such as nanoparticle concentrations, flow Reynolds number, type of base fluid and heat flux are investigated. The following conclusions are drawn from the results of experiments in this study:

- Addition of nanoparticles into the base fluid enhances the convective heat transfer coefficient and the enhancement increases with increasing particle concentration.
- The enhancement due to addition of nanoparticles seems to be more considerable in the high Reynolds number.
- Enhancement of the convective heat transfer coefficient for the mixture consisting of 60 weight-% ethylene glycol and 40 weight-% distilled water is more than the nanofluid of distilled water.
- The use of TiO_2 nanoparticles as the dispersed phase in distilled water can significantly enhance the convective heat transfer and the enhancement increases with increasing heat flux.
- good agreement between experimental data and predicted results of ANN shows that ANN can be used to model this process with high accuracy except for higher heat flux.

References

1- Pak, B.C. and Cho, Y.I., (1998) Hydrodynamic and heat transfer study of dispersed fluids with submicron metallic oxide particle, Exp. Heat Transfer, 11, PP. 151–170.

2- He, Y., Men, Y., Zhao, Y., Lu, H. and Ding, Y., (2009) Numerical investigation into the convective heat transfer of TiO_2 nanofluids flowing through a straight tube under the laminar flow conditions, Appl. Therm. Eng., 29, PP. 1965-1972.

3- A. K. Santra, N. Chakraborty, S. Sen, Prediction of heat transfer due to presence of copper–water nanofluid using resilient-propagation neural network, International Journal of Thermal Sciences, 48 (2009) 1311–1318.

4- Fazeli, S. A., Hosseini Hashemi, S. M., Zirakzadeh, H., Mehdi Ashjaee, Experimental and numerical investigation of heat transfer in a miniature heat sink utilizing silica nanofluid, Superlattices and Microstructures, 51 (2012) PP. 247–264

5- M. Balcilar, A.S. Dalkilic, A. Suriyawong, T. Yiamsawas, S. Wongwises, Investigation of pool boiling of nanofluids using artificial neural networks and correlation development techniques, International Communications in Heat and Mass Transfer, 39 (2012) 424–431V.

6- M. M. Papari, F. Yousefi, J. Moghadasi, H. Karimi, A. Campo., Modeling thermal conductivity augmentation of nanofluids using diffusion neural networks, International Journal of Thermal Sciences, 50 (2011) 44e52.

7- M. Hojjat, S.Gh. Etemad, R. Bagheri, J. Thibault, Thermal conductivity of non-Newtonian nanofluids: Experimental data and modeling using neural network, International Journal of Heat and Mass Transfer, 54 (2011) 1017–1023.

8- Hamilton, R.L. and Crosser, O.K., (1962) Thermal conductivity of heterogeneous two-component systems, I&EC Fundam. 125 (3), PP. 187–191.

9- Gnielinski, V., (1976) New equations for heat and mass transfer in turbulent pipe and channel flow, Int. Chem. Eng., 16, PP. 359-368.

10- Shah R. K, (1975) Thermal entry length solutions for the circular tube and parallel plates, Proc. 3th Intl. Heat Mass Trans. Conf., PP. 11-75.

11-. A.B. Bulsari, Neural networks for chemical engineers (Elsevier Science Inc., New York, 1995)

Figure captions

Fig. 1. Experimental Apparatus

Fig. 2. Comparison of the measurements with the Gnielinski equation for distilled water flows. (a) Re = 2960 and (b) Re = 3960.

Fig. 3. Axial profiles of heat transfer coefficient of nanofluids at different TiO_2 nanoparticle concentrations in the turbulent flow regimes of water on the base of experimental data and ANN results. (a) Re = 2960 and (b) Re = 3960.

Fig. 4. Comparison of the measurements with the Shah equation for mixture of water and ethylene glycol flows at Re = 2030.

Fig. 5. Axial profiles of heat transfer coefficient of nanofluids at different TiO_2 nanoparticle concentrations in the mixture consisting of 60 weight-% ethylene glycol and 40 weight-% distilled water on the base of experimental data and ANN results.

Fig. 6. Effect of heat flux on the convective heat transfer coefficient of nanofluid in different TiO_2 nanoparticle concentrations on the base of experimental data and ANN results.

Figure 1:

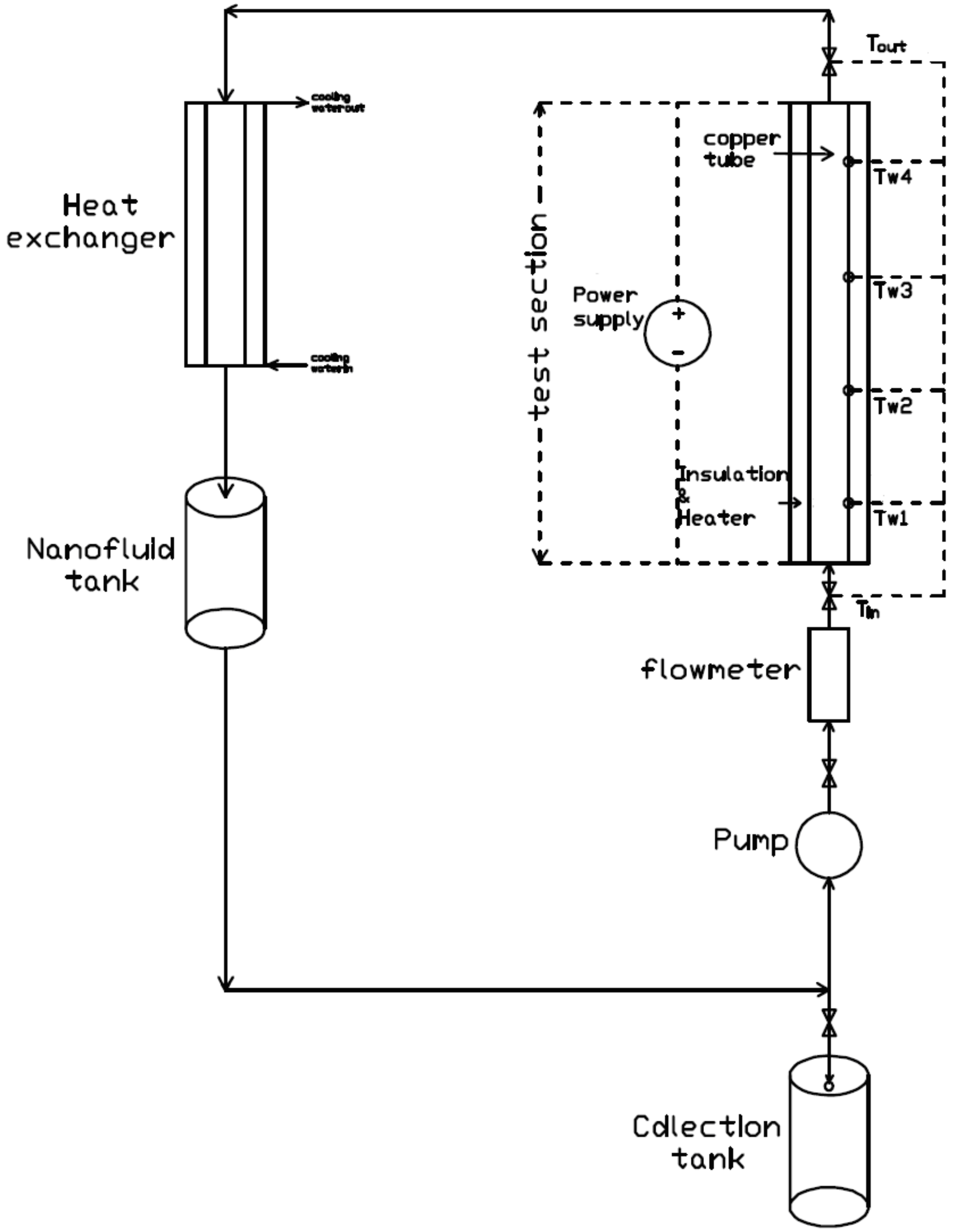
Tout
cooling
waterout
Heat
exchanger
copper
tube
Tw4
test section
Tw3
Power
supply
+
-
cooling
waterin
Tw2
Insulation
&
Heater
Tw1
Nanofluid
tank
Tin
flowmeter
Pump
Collection
tank

Figure 2:

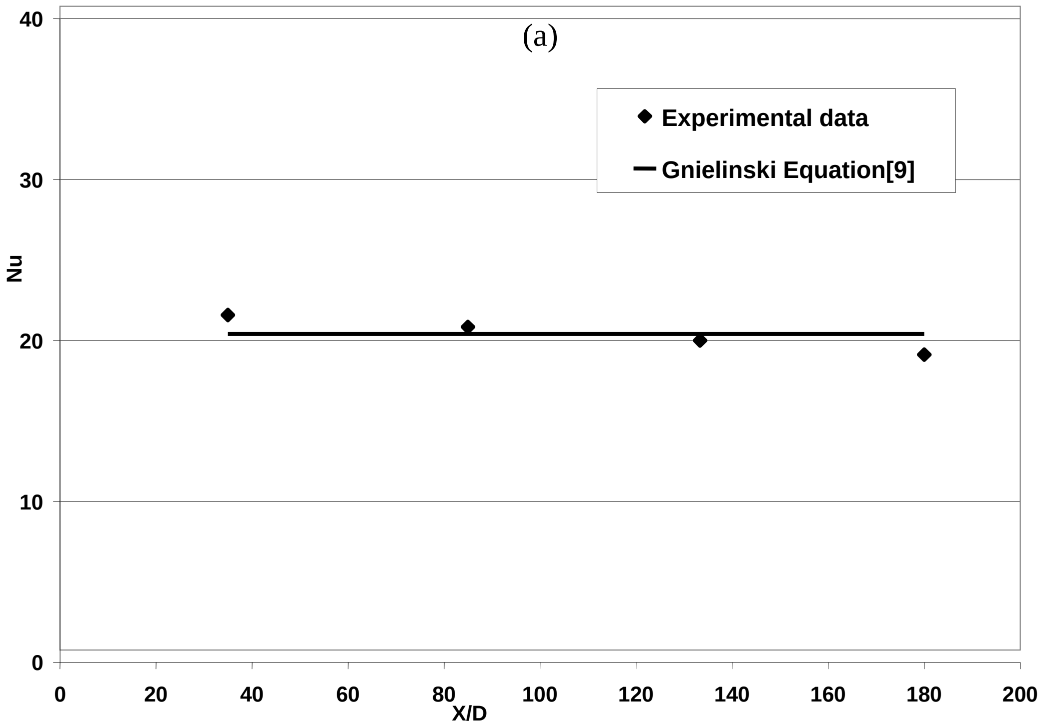

(a)
Experimental data
Gnielinski Equation[9]
Nu
X/D
0
10
20
30
40
0
20
40
60
80
100
120
140
160
180
200

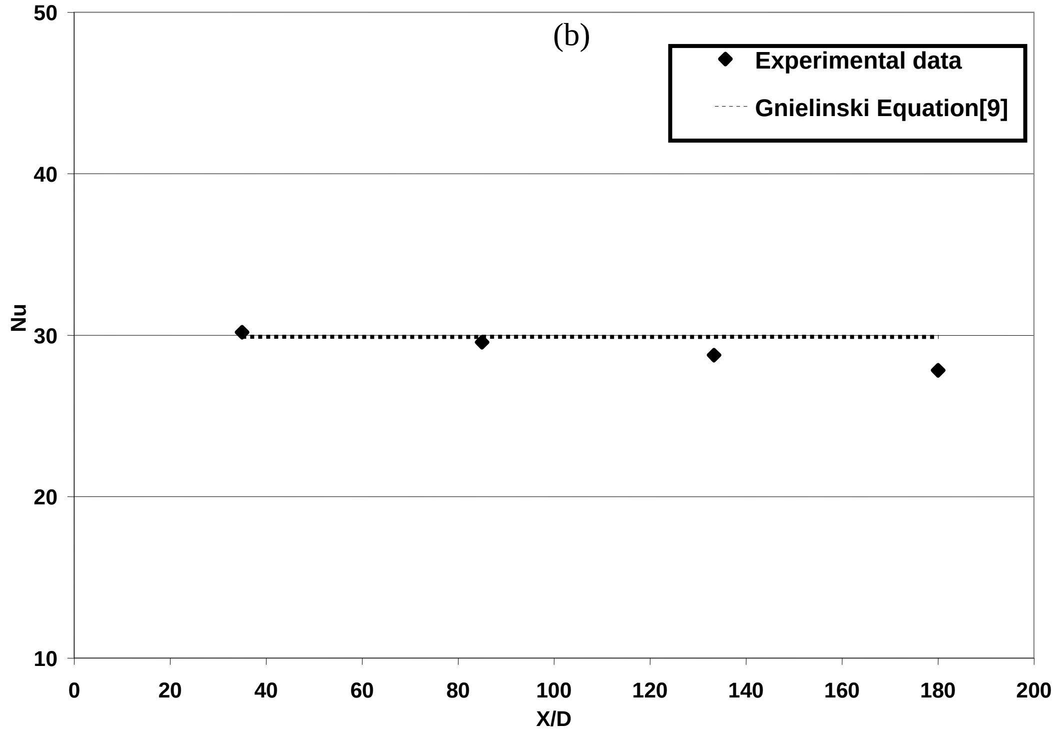

(b)
Experimental data
Gnielinski Equation[9]
Nu
X/D
10
20
30
40
50
0
20
40
60
80
100
120
140
160
180
200

Figure 3:

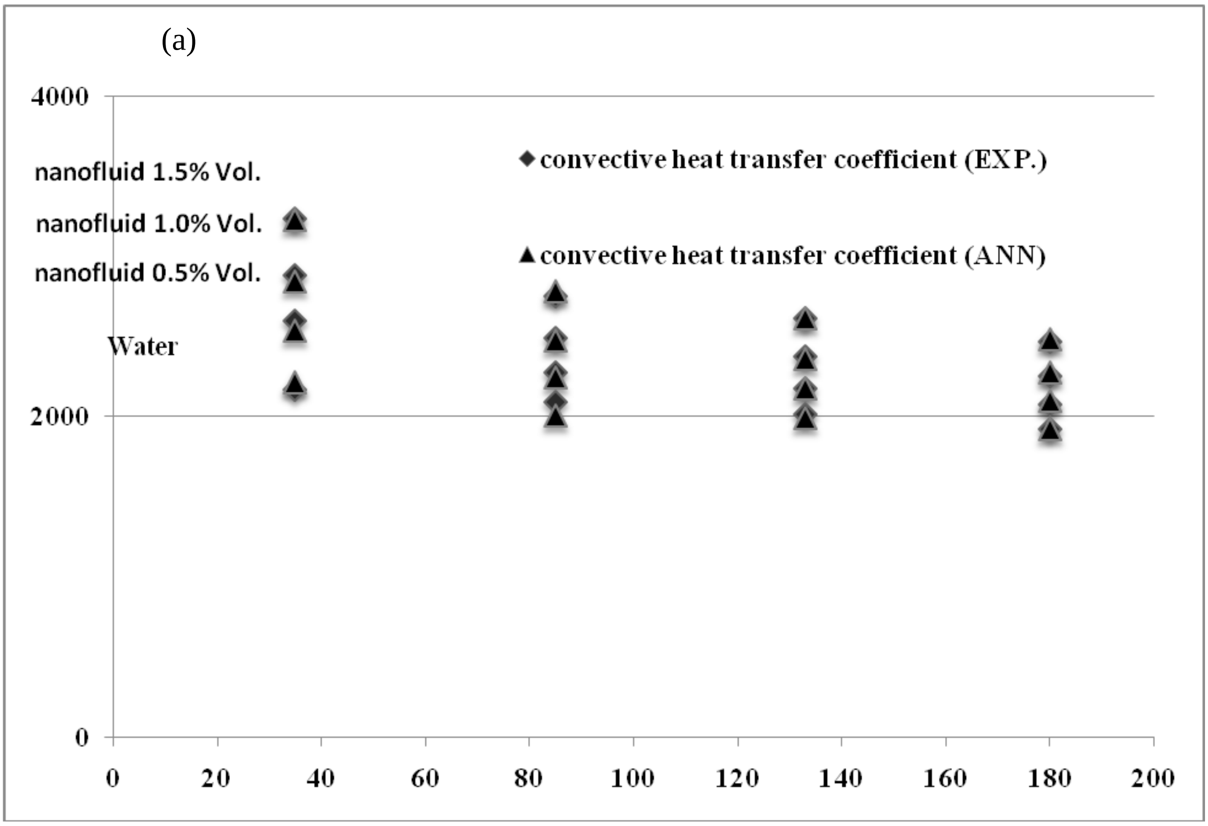

(a)
4000
2000
0
nanofluid 1.5% Vol.
nanofluid 1.0% Vol.
nanofluid 0.5% Vol.
Water
convective heat transfer coefficient (EXP.)
convective heat transfer coefficient (ANN)
0
20
40
60
80
100
120
140
160
180
200

(b)

▲ heat transfer coefficient (ANN)

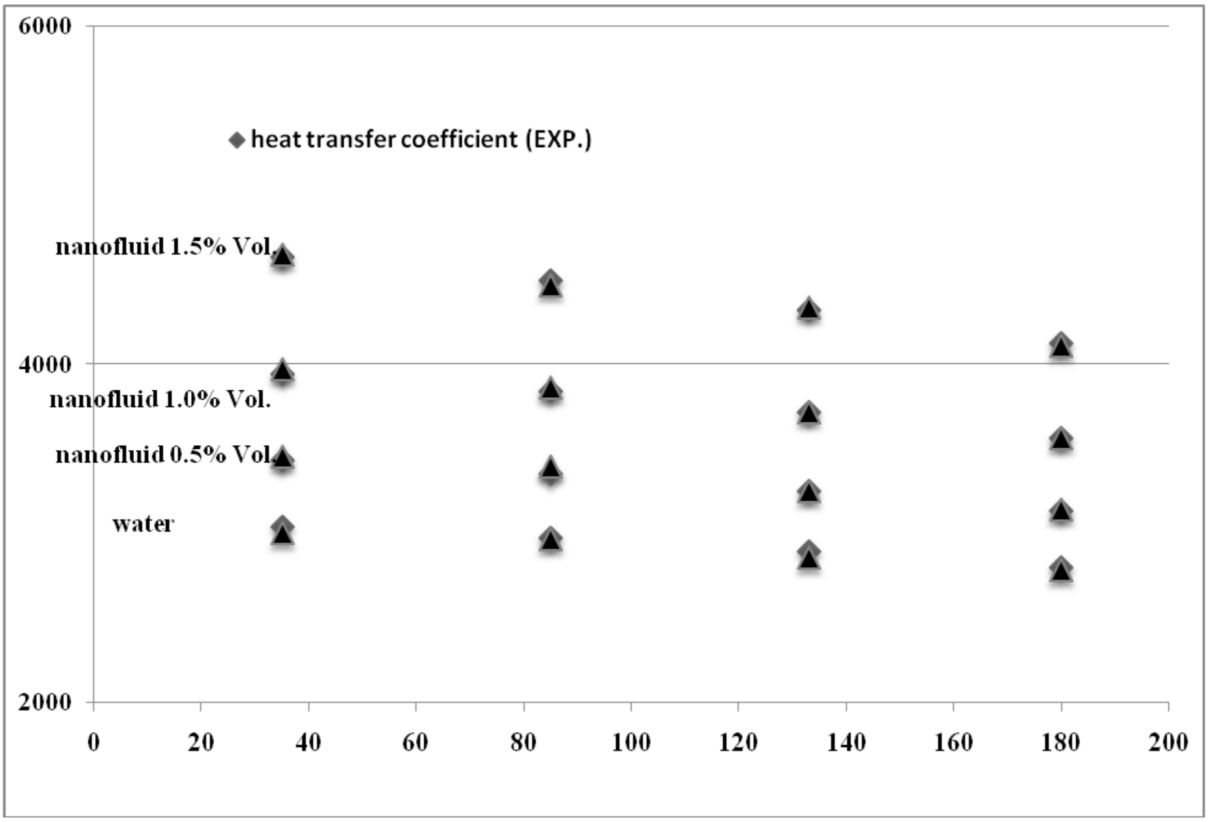

Figure 4:

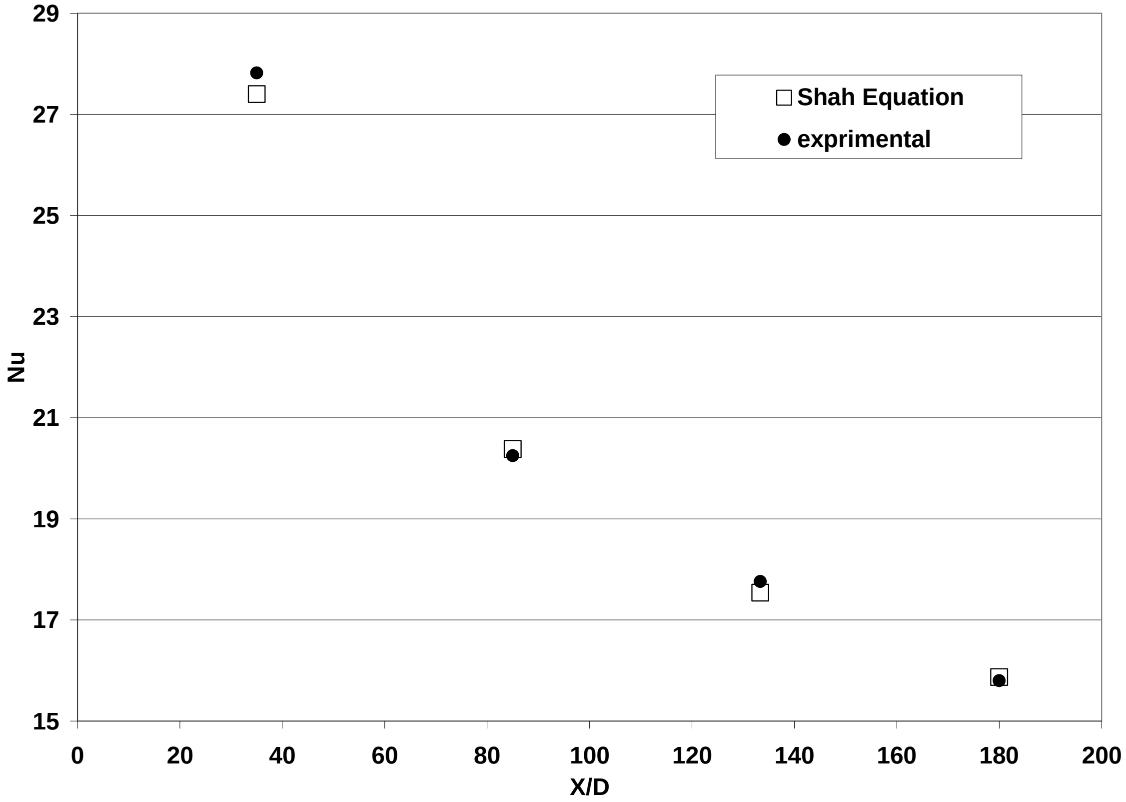
Shah Equation
exprimental
Nu
X/D
29
27
25
23
21
19
17
15
0
20
40
60
80
100
120
140
160
180
200

Figure 5:

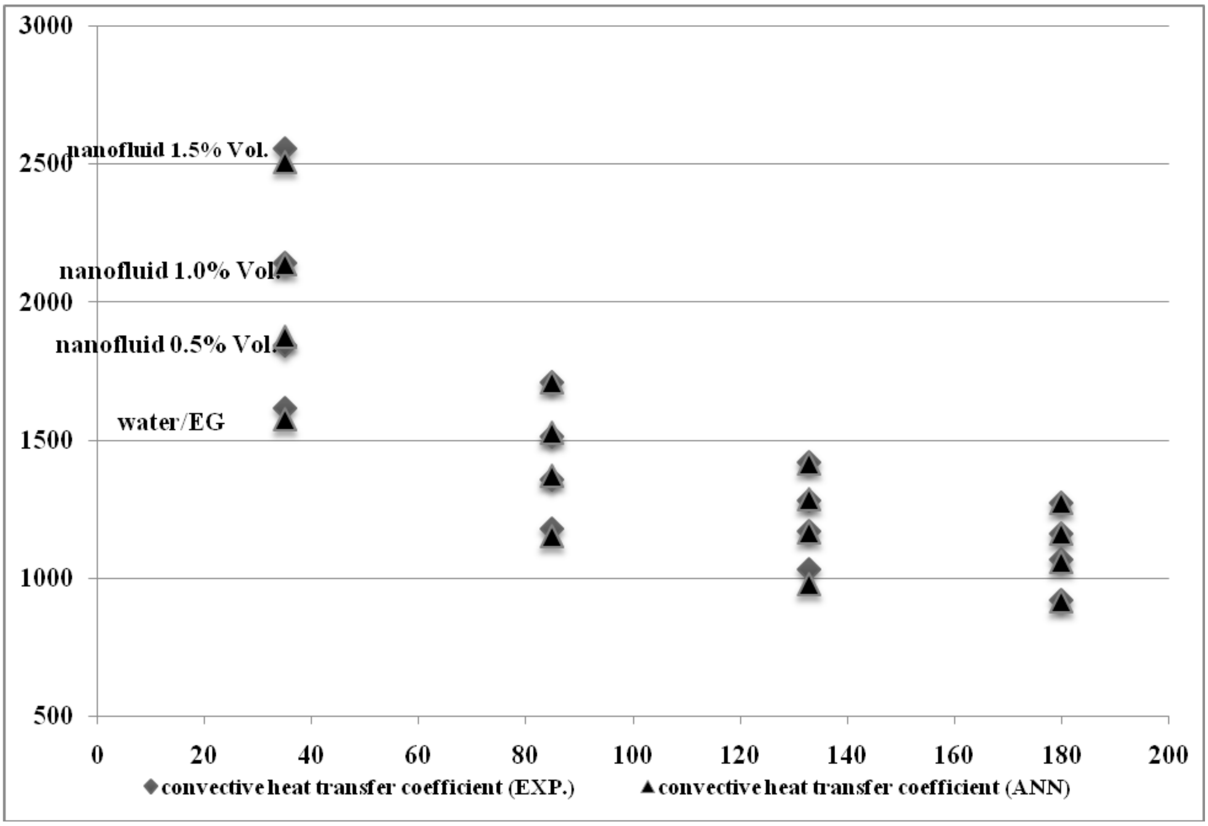

3000
2500
2000
1500
1000
500
0
20
40
60
80
100
120
140
160
180
200
nanofluid 1.5% Vol.
nanofluid 1.0% Vol.
nanofluid 0.5% Vol.
water/EG
convective heat transfer coefficient (EXP.)
convective heat transfer coefficient (ANN)

Figure 6:

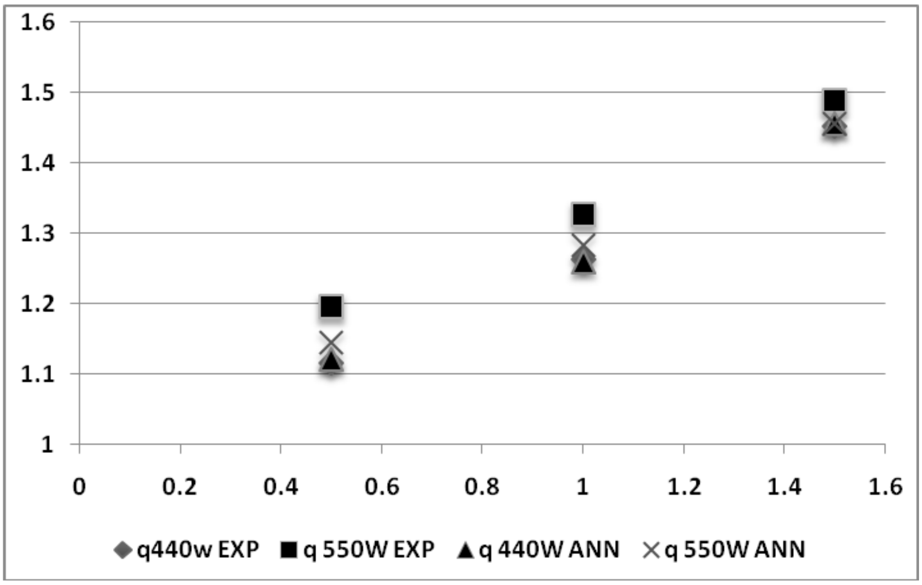

Table 1. Comparison of various back propagation learning algorithms

Back propagation (BP) algorithm	**function**	**MSE**	**R^2**
Resilient backpropagation (Rprop)	trainrp	0.0099	0.9899
Fletcher–Reeves conjugate gradient backpropagation	traincgf	0.0031	0.9969
Polak–Ribi´ere conjugate gradient backpropagation	traincgp	0.0042	0.9957
Powell–Beale conjugate gradient backpropagation	traincgb	0.0039	0.9960
Levenberg–Marquardt backpropagation	trainlm	**0.0010**	**0.9990**
Scaled conjugate gradient backpropagation	trainscg	0.0112	0.9944
BFGS quasi-Newton backpropagation	trainbfg	0.0037	0.9963
One step secant backpropagation	trainoss	0.0042	0.9957
Batch gradient descent	traingd	0.0089	0.9910
Vairable learning rate backpropagation	traingdx	0.2186	0.7778
Batch gradient descent with momentum	traingdm	0.1061	0.8963

Table 2. Number of neurons in hidden layer with related mean square errors.

Number of neurons	MSE×10^2
2	1.69
3	0.31
4	0.23
5	0.17
6	**0.08**
7	0.20
8	0.11
9	0.15